ADVANCED ENGINEERING MATERIALS
www.aem-journal.com

The Effect of Residual Stresses on Stress–Strain Curves Obtained via Profilometry-Based Inverse Finite Element Method Indentation Plastometry

*Max Burley, Jimmy E Campbell, Rebecca Reiff-Musgrove, James Dean, and Trevor William Clyne**

This paper concerns, the effect of (unknown) residual stresses in the near-surface region of a sample on outcomes of an indentation plastometry technique for obtaining stress–strain relationships, using relatively large spherical indenters. The technique is based on the iterative finite element method (FEM) simulation of indentation, so as to infer the true stress–strain curve of the material (with the target outcome being the profile of the residual indent). It is expected that residual stress levels (if significant compared with the yield stress) are likely to influence the outcome, and indeed this forms the basis of many attempts to measure residual stresses in this way (using a known stress–strain curve). However, there are important issues of sensitivity here, which affect the reliability of such procedures and are also relevant to the accuracy of stress–strain curves inferred from measurements made on samples containing unknown levels of residual stress. Herein, both experimental work on samples with (equal-biaxial) residual stresses created by the application of external loads and extensive FEM modeling to explore various scenarios are covered. The main conclusion is that the sensitivities involved are in general very low, particularly with relatively deep indentation. Inferred stress–strain curves are thus likely to be quite accurate, even in the presence of relatively high levels of residual stress. Conversely, the measurement of residual stress levels via this procedure is likely to be rather inaccurate, although the reliability is improved using shallow penetration (low ratio of depth-to-indenter radius). It is also noted that tensile residual stresses tend to influence outcomes more strongly than compressive ones.

1. Introduction

1.1. Obtaining Stress–Strain Curves from Indentation Data

Two main approaches have been adopted for extraction of stress–strain curves from indentation data. The first, which has commonly been termed "instrumented indentation technique" (IIT), seeks to simply convert load–displacement data directly to a stress–strain curve, using analytical relationships. This inevitably involves gross simplifications concerning the actual stress and strain fields under the indenter, although it is very attractive in terms of the ease and speed of obtaining the final outcome. Most IIT methodologies are based on repeated interruption, partial unloading, and reloading during the test. A wide range of analytical formulations have been proposed for obtaining the effective values of stress and strain at each point. These are reviewed in several publications.[1–5]

The second is a more rigorous approach, although inevitably more cumbersome. It is based on iterative finite element method (FEM) simulation of the indentation process, systematically changing the values of the parameters in a constitutive plasticity law until optimum agreement is reached between a measured and a modeled outcome—either the load–displacement plot or the residual indent profile. The latter is now often preferred[6–9] and in this case the procedure can be described as "profilometry-based inverse FEM indentation plastometry" (PIP). Unlike IIT procedures, no approximations are required concerning the mechanics of indentation. However, several questions surround its practicality, efficiency, and reliability. Various publications[10–15] have addressed the issues that have to be taken into account. The three basic steps involved are 1) pushing a hard indenter into the sample with a known force, 2) measuring the experimental outcome, i.e., the (radially symmetric) profile of the indent (although most early work was based on the load–displacement plot), and 3) iterative FEM simulation of the test, systematically changing the set of plasticity parameter values until optimal agreement is obtained between measured

Dr. M. Burley, Dr. J. E. Campbell, Dr. J. Dean, Prof. T. W. Clyne
Plastometrex Ltd
204 Science Park, Cambridge CB2 0GZ, UK
E-mail: b.clyne@plastometrex.com

R. Reiff-Musgrove, Prof. T. W. Clyne
Department of Materials Science
27 Charles Babbage Road, Cambridge CB3 0FS, UK

The ORCID identification number(s) for the author(s) of this article can be found under https://doi.org/10.1002/adem.202001478.

DOI: 10.1002/adem.202001478

and modeled outcomes. The underlying concept is thus clear and unencumbered by uncertainty about the validity of the procedure. However, for it to be a tool of widespread utility, concerns have to be addressed relating to the rate of convergence (in parameter space) on the "solution",[14–19] the possibility that it is not "unique", the resolution requirements for the experimental outcome, etc. It has already been applied using a commercially available integrated product to study industrial cases.[9,20,21] Also, a systematic comparison[22] between the outcomes of applying IIT and PIP procedures to several different materials clearly revealed the superior reliability of the latter.

Important points concerning optimization of the PIP procedure include the attractions of a spherical indenter[14] and the requirement to deform a volume that is large enough for its mechanical response to be representative of the bulk. This requires it to be a "many-grain assembly" and typically translates into the need for the indenter radius to be of the order of 1 mm and the load capability to extend to the kN range. An integrated facility incorporating an indenter, a profilometer, and associated control and analysis software is now being sold commercially by Plastometrex Ltd and this was used in the work described here.

1.2. Effects of Residual Stress

It has long been clear that, during indentation, the presence of residual stress in the near-surface region can affect the way that plasticity develops and hence the details of the penetration characteristics (load–displacement plot and residual indent profile). A potential attraction of PIP-type procedures (based on FEM simulation of the test) is that it is a simple matter to incorporate any given set of residual stresses into the model. As indentation is normally conducted to a relatively shallow depth, and in a region of limited lateral extent, any variations in the residual stress state within the region being tested can be neglected. Of course, there is scope for mapping changes in residual stress over the surface of a sample by making indents in different locations. Furthermore, since there can be no stress normal to a free surface, the residual stress state in an indentation-tested region is fully characterized by the two (in-plane) principal stresses. In some cases, these two principal stresses will be the same, so that only a single value has to be obtained. Otherwise, three parameters are needed, two being values of the two principal stresses and the third specifying their orientation.

Certain expected features can be identified quite easily. Indenting initially creates mainly a compressive stress in the through-thickness direction. Yielding will occur when the difference between this and the initial in-plane stress reaches the yield stress. Initial yielding will thus clearly be promoted by a tensile residual stress and inhibited by a compressive one, with the effect expected to be stronger with tensile stresses. Of course, as penetration proceeds, the stress field becomes more complex, but the trends are still expected to be in the same direction, and some asymmetry is likely to remain in terms of the magnitude, as well as the sense, of the effects with the two types of residual stress. There is further complexity with unequal-biaxial residual stresses, but a key question is whether the sensitivities are such that inferring residual stresses in this way is likely to be practicable. Of course, profilometry has potential for establishing the directionality of any anisotropy in the residual stress state, whereas this is not possible if attention is focused on load–displacement data.

A key objective is capability to infer the residual stress state from an experimental indentation outcome, presumably with the true stress–true strain relationship of the material already known. There have in fact been many studies aimed at measuring residual stresses via indentation, although no clear and viable methodology has emerged so far. A sizeable proportion of these studies have been oriented toward the effect of residual stresses on hardness. The ill-defined nature of hardness means that such approaches do not really have any potential in terms of experimental measurement of residual stresses. However, a number of others[23–35] have focused on monitoring how indenter penetration is affected by residual stresses. These investigations have all concerned metals, although similar procedures have been applied to polymers.[36] A number of these studies have been purely theoretical, but some have involved experimental indentation of samples in which controlled "artificial" residual stresses have been created by the external application of (equal- or unequal-biaxial) forces[31,32,34,35,37] or via differential thermal contraction between a substrate and a surface layer.[26]

The most relevant of these for current purposes are those involving relatively large spherical indenters.[28,30,32–35] These include the work of Peng et al.,[32,35] who showed that changes in experimental load–displacement plots induced by imposing "residual" stresses via externally applied loads were consistent with FEM predictions. Of course, load–displacement plots cannot be used to infer anisotropic residual stress states, as they provide no directional information. The authors did, however, view the residual indents optically, noting that their shapes became (approximately) elliptical when the residual stresses were unequal. On the other hand, they neither measured indent profiles, nor used iterative FEM to infer residual stress states. Furthermore, they assumed that the "residual" stress in the centre of their cruciform samples (where the indentation was conducted) was equal to the applied load over the sectional area of the "arm": as shown below, this is an inaccurate assumption. Other relevant work includes that of Zhang et al.,[30,34] who explored the effect of using different constitutive laws for plasticity and confirmed that the changes induced in the load–displacement plot by the presence of residual stresses can be significant. Finally, Wang et al.[33] proposed a method for extracting both the plasticity parameters and the residual stress characteristics, using multiple indent depths.

There has therefore been no previous work involving the application of inverse FEM to residual indent profiles, for material with known plasticity characteristics, so as to infer the nature and magnitude of (externally imposed) residual stresses. The present work includes such a study, focusing on equal-biaxial stresses (both tensile and compressive) created in thin sheet samples. However, the real objective is to explore the sensitivities involved, i.e., to quantify the effect of particular levels of residual stress on the experimental outcome (residual indent profile). This gives insights, not only into the probable accuracy of inferred levels of residual stress, but also into the levels of error likely to be introduced into the stress–strain curve obtained via PIP by the (unknown) presence of residual stresses.

2. Experimental Section

2.1. Specimen Production

The obvious way to create a well-defined (biaxial) state of "residual" stress is to apply external loads in two orthogonal directions to a cruciform-shaped sample. Provided that the applied stresses are kept below the yield stress, this should have no effect on the (true) stress–strain relationship that the material will exhibit during indentation (which can be established via conventional tensile testing). Furthermore, with a fairly thin sample, it should be possible to create a state of residual stress that is uniform in depth and keep the applied load within a manageable range. Similar configurations have been used in previous investigations.[31,35] In the present work, samples were made by machining a 3 mm-thick sheet of OFHC copper (grade C106), supplied by Doré metals. The dimensions of the design are shown in **Figure 1**.

Samples for conventional uniaxial tensile testing were produced in a similar way, having a gauge length of 56 mm, where the width was 8 mm, grip section 30 mm long and 16 mm wide, and a radius 4 mm in the shoulder region. Tensile testing was conducted using an Instron screw-driven testing machine, under displacement control, at a rate of 10 mm min^{-1}.

It is, of course, possible that the samples initially contained residual stresses—perhaps from the original rolling process. This should have no significant effect on tensile testing, as any such stresses must force balance to zero over the complete thickness of the sample. The near-surface regions could in principle contain net residual stress, and these could influence indentation outcomes. In practice, any such stresses are likely to be low in this case. In any event, the indentation procedure is effectively interrogating a region that extends more or less to the midplane of the sample and this region also is expected to have a null force balance.

2.2. Cruciform Sample Loading Configuration

The state of stress in the sample must be not only accurately controllable but also uniform laterally over the region to be indented.

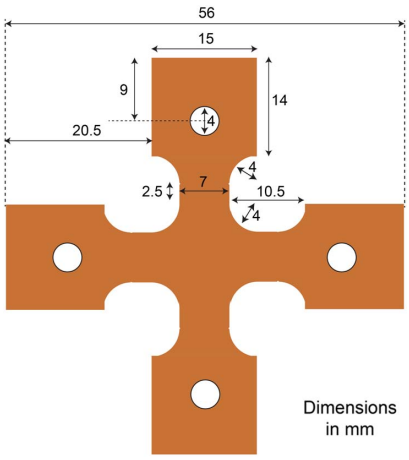

Figure 1. Dimensions of the cruciform samples.

This requires care in the design of the sample and gripping system. **Figure 2** shows a schematic depiction of the loading frame, which is similar to that by Peng et al.[35] The thickness of the frame was 40 mm. The loads were applied by tightening of the nuts (creating either compression or tension in the sample). The load was transmitted to the sample via "load transmission rods" and bolts through the holes in the sample. The magnitude of the applied load was monitored via strain gauges on the transmission rods and also via the torque being applied to the nut. The transmission rods had a relatively small load-bearing sectional area in the region where the strain gauge was located—they were 20 mm wide—but there was a central cavity, leaving residual 3 mm-thick layers top and bottom. The load-bearing section there was thus $20 \times 6 = 120\ mm^2$. This led to relatively large strain gauge readings for a given load. These readings ranged up to about 500 microstrain, corresponding to a stress of about 35 MPa (so the forces applied ranged up to about 4 kN). This stress level was well below the yield stress of aluminum, which was a few hundred MPa. In the current work, only equal-biaxial stresses were applied, although the rig can evidently also be used for cases in which the two stresses are different (including cases where they are of opposite sign).

2.3. Simulation of Cruciform Sample Loading

To explore the relationship between the applied loads (as measured via the strain gauges on the transmission rods) and the resultant stress state in the region of the sample to be indented, a 3D FEM model was set up, based on the mesh shown in **Figure 3**. The loading boundary condition was that a force was applied to the inner surface of the hole (created by a bolt that fitted closely into it). In a particular direction, one of the pair of holes remained stationary while the other was displaced: this created some asymmetry between the two sides of the sample, although this was relatively small.

An outcome of this type of modeling is shown in **Figure 4**, which refers to a particular equal-biaxial tensile case. An

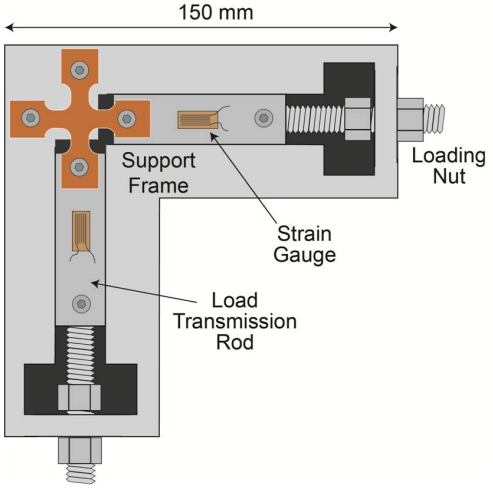

Figure 2. Depiction of the loading frame used to create the residual stresses in the sample. The frame and transmission rods are made of aluminum.

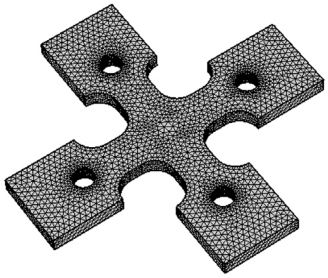

Figure 3. FEM mesh for simulation of the stress state within cruciform samples.

immediate point to note here is that both the von Mises stress and the axial stress(es) have a significantly different magnitude in the central region (to be indented) than in the "arms" of the sample. The nominal stress in the arms (given by the load over the sectional area) was in this case about 181 MPa. It can be seen that the stresses (in both directions) in the central region were well below this value. This effect is a consequence both of the geometry of the sample (the effective sectional area being higher in the centre) and of Poisson effects. This is important, as an error would arise if the stress in the center is simply taken to be the load divided by the sectional area of the arms, as was apparently assumed in the work of Peng et al.[35]

Some details of the effect are shown in **Figure 5**, which is a plot of the variation with axial location of the von Mises stress and the two axial stresses, for the case shown in Figure 4. The main focus here is on the von Mises stress. Two points may be noted. The first is that the von Mises stress in the central region is not much more than half of the value in the arms (i.e., the applied load over the sectional area of the arms, which was 7 mm by 3 mm). The other is that the level in the central 5 mm or so is approximately uniform. This region is sufficiently large to cover virtually the whole of the volume that is plastically deformed during indentation (as required). In fact, as the average value is about 110 MPa, and behavior in this regime is linear elastic, the von Mises stress created in the region to be indented is given by $110F/3.8$, where F is the (equal-biaxial) applied force in kN.

2.4. Indentation Plastometry

Three steps are involved in obtaining a true stress–strain curve from an indentation test. These are 1) pushing a hard indenter into the sample with a known force, P, 2) measuring the (radially symmetric) profile of the indent, and 3) iterative FEM simulation of the indentation until the best fit set of plasticity parameter values is obtained. A crosscheck can be made with the outcome of a conventional tensile test (a nominal stress–strain plot) by running an FEM simulation of the test, using the derived true stress–strain relationship. (If interest is limited to the regime up to the onset of necking, then the standard equations can be used to relate nominal and true stress–strain curves, so that no FEM simulation of the tensile test is needed.) The Voce

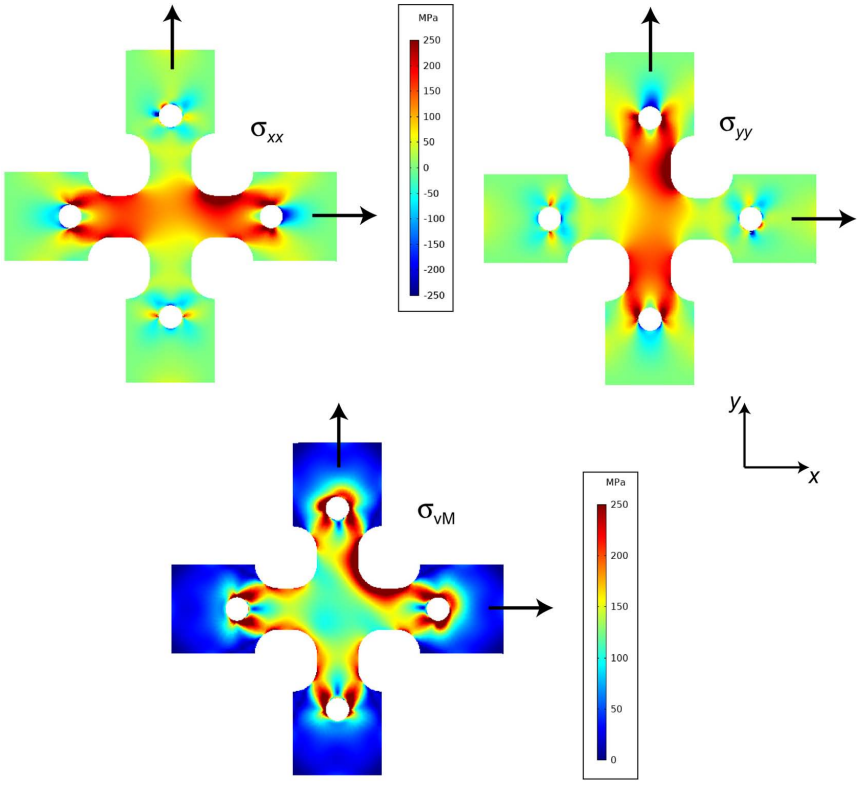

Figure 4. FEM-predicted stress fields in a cruciform sample subjected to a load of 3.8 kN in both x- and y-directions, via the displacement of bolts acting through two of the holes.

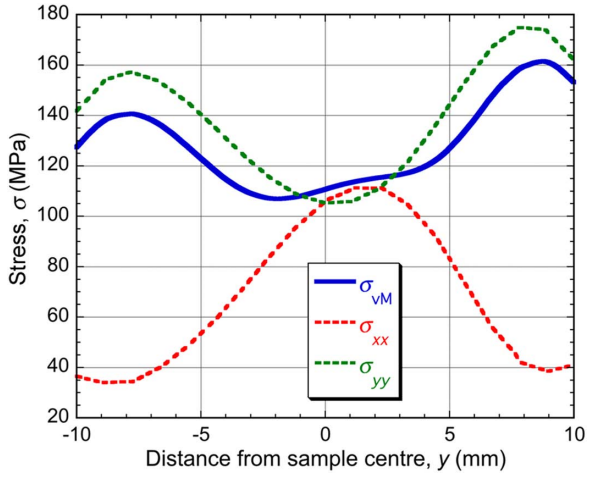

Figure 5. Outcome of FEM simulation of the stress state within a cruciform sample, with two applied loads of 3.8 kN, showing the variation with axial position (along the *y*-axis) of the von Mises stress and the two axial stresses.

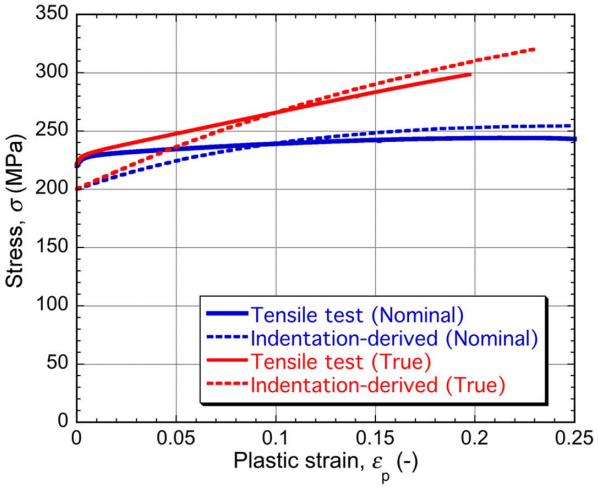

Figure 6. A comparison between the stress–strain curves obtained by conventional tensile testing and by indentation plastometry.

constitutive law was used to capture the plasticity. Details are available elsewhere.[9]

In the present work, there was a further operation of measuring profiles after indentation with imposed (equal-biaxial) residual stresses and then conducting iterative FEM simulation with different values of this imposed stress until convergence (best fit) is achieved. As there was only a single unknown parameter (the imposed stress), this convergence operation was straightforward, simply involving selection of the value and giving the best fit between modeled and measured profiles (i.e., the lowest value of the misfit parameter, S_{red}). The residual stress level inferred in this way can then be compared with the actual value.

3. Indentation and Tensile Testing Outcomes

3.1. Behavior with No Residual Stress

The first step in the approach being adopted is to be clear about the plasticity characteristics of the material. A comparison is shown in **Figure 6** between the stress–strain curves obtained by conventional tensile testing and indentation plastometry. (Both tensile tests and indentation runs were repeated several times and the reproducibility was found to be good, i.e., around ±5%.) For the tensile test, the original data are those of the nominal stress–strain plot, which have been converted to a true stress–strain plot using the standard equations (which can be done only up to the onset of necking at about 20% nominal strain). The original outcome of the indentation plastometry is an inferred true stress–strain curve. The values of the Voce plasticity parameters, and the corresponding value of the misfit parameter, are shown in **Table 1**.

The true stress–strain curve in Figure 6 is simply a plot of the Voce equation, using these values. This curve has been converted to a nominal one, using the same analytical relationships that were used in converting the tensile nominal plot to a true one. (For present purposes, there is no interest in the postnecking behavior in a tensile test.) It can be seen that the agreement is good, with a yield stress of about 200–220 MPa and relatively little work hardening, such that the UTS is about 250 MPa. The reproducibility was about ±5% for both types of tests. The yield stress level should be noted, as the imposed "residual" stress has to be kept well below it. It may also be noted that both tensile testing and measuring indentation profiles in different in-plane directions gave very similar outcomes, so it can be concluded that the material does not exhibit any significant (in-plane) anisotropy.

3.2. Indentation with Residual Stresses

3.2.1. Experimental Outcomes

Figure 7 shows a set of experimentally measured residual indent profiles, obtained with a range of superimposed (equal-biaxial) residual stresses. Using the formula given in §2.3, these values (expressed as a von Mises stress) are about −101 MPa, −57 MPa, 0, +54 MPa, and +110 MPa. (These values are all well below the yield stress of about 200 MPa.) The two sets of curves correspond to two different values of the indentation load *P*. The value of *P* is usually chosen so as to give a suitable penetration ratio (indentation depth over indenter radius). In general, this should be of the order of 20%, so as to generate plastic strains in approximately the required range. It can be seen that this is the case in Figure 7b, with $P = 1.0$ kN, but the penetrations were lower in

Table 1. Outcome of the convergence operation on the residual indent profile (in the absence of residual stress) to infer the true stress–strain relationship (parameter values in the Voce law).

Best fit Voce parameter values			
Yield stress, σ_Y [MPa]	Saturation stress, σ_s [MPa]	Characteristic strain, ε_0 [%]	Misfit parameter, S_{red} [–]
200	400	25	5.3×10^{-5}

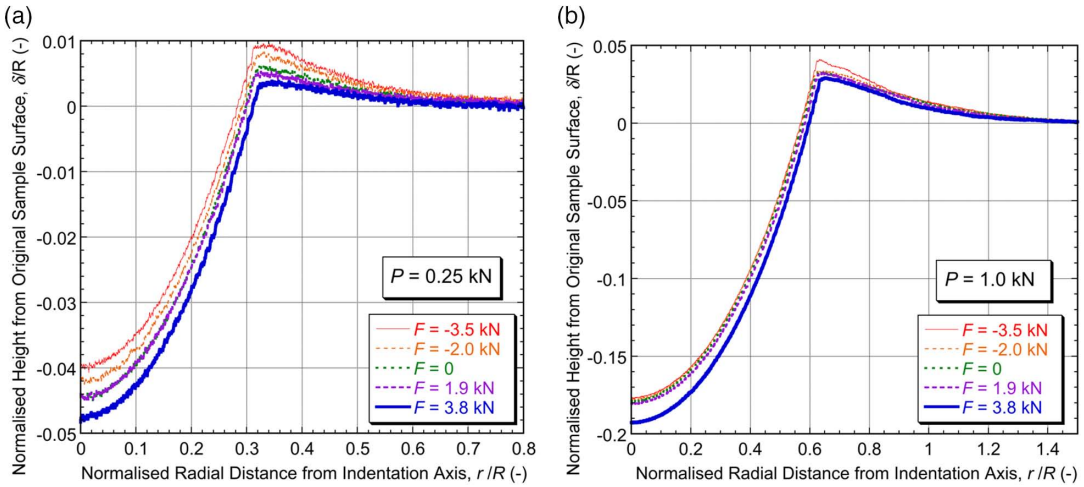

Figure 7. Experimentally measured indent profiles for five values of the applied (biaxial) force, F, for an indentation load, P, of a) 0.25 kN and b) 1.0 kN.

Figure 7a, for which $P = 0.25$ kN. This has been done to illustrate a point about sensitivities.

The general nature of the effect is as expected in both cases, with tensile stress promoting penetration and compressive stress inhibiting it. However, in relative terms, the differences between the curves with different residual stress levels are rather greater for the shallower penetration. As the indenter goes deeper, the stress field becomes more complex, with more lateral movement of material and the stress field from the indentation load departing from the initial situation, in which it is largely compressive stress in the loading direction. For deeper penetration, the effect of the residual stress level starts to reduce, particularly for the compressive ones.

3.2.2. FEM Simulation

The FEM model set up for indentation of residually stressed samples was radially symmetric, with an initial residual radial stress equal to the von Mises stress level indicated by the (3D) modeling of the cruciform samples. Predicted indent profiles are compared with the experimental ones in **Figure 8**, for three of the residual stress levels (including zero). Of course, for the unstressed case, the agreement is good (as the plasticity parameter values have been selected to give optimal fit). For the two residually stressed cases, however, it is relatively poor (with deep penetration).

This relatively poor agreement merits investigation, as it carries an implication that the inverse operation is likely to result in erroneous inferred stress levels. **Figure 9** shows fields of radial stress with an indentation load, P, of 1.0 kN, with and without an initial (residual) radial stress of +115 MPa. Comparing these two gives some insights into how residual stresses affect the indentation process. In fact, despite the fact that tensile stresses influence the indentation more strongly than compressive ones, it can be seen that, at least by the stage shown (at which the penetration has reached the levels normally used, i.e., $\delta/R \approx 20\%$), the effect of this prior stress on the stress field around the indent is small. This is also true of the von Mises stress field. This suggests that the sensitivity of the indentation characteristics to the residual stress level is also likely to be small.

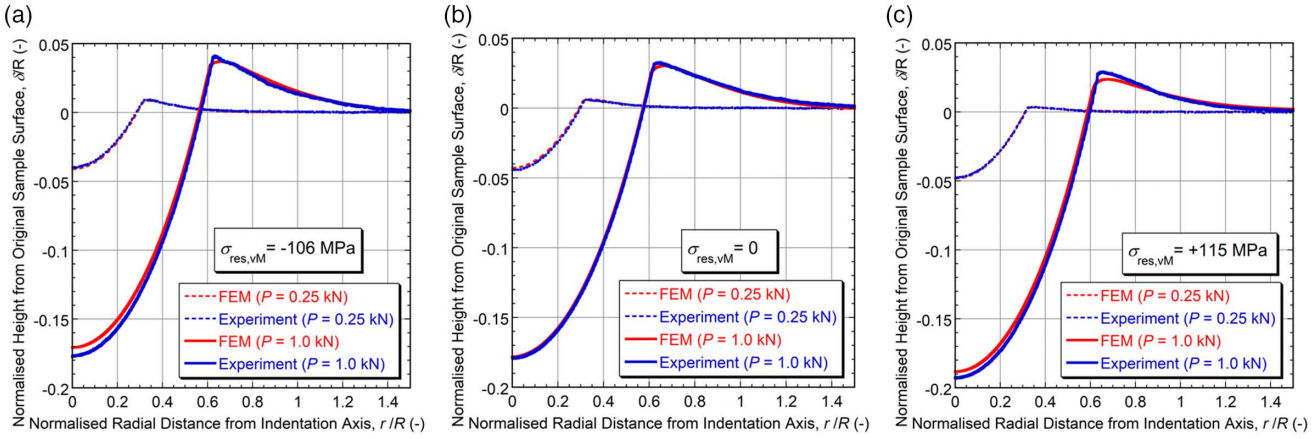

Figure 8. A comparison between experimental and FEM-modeled indent profiles with two values of the indentation load, P, for residual von Mises stresses of a) −101 MPa, b) 0, and c) +110 MPa.

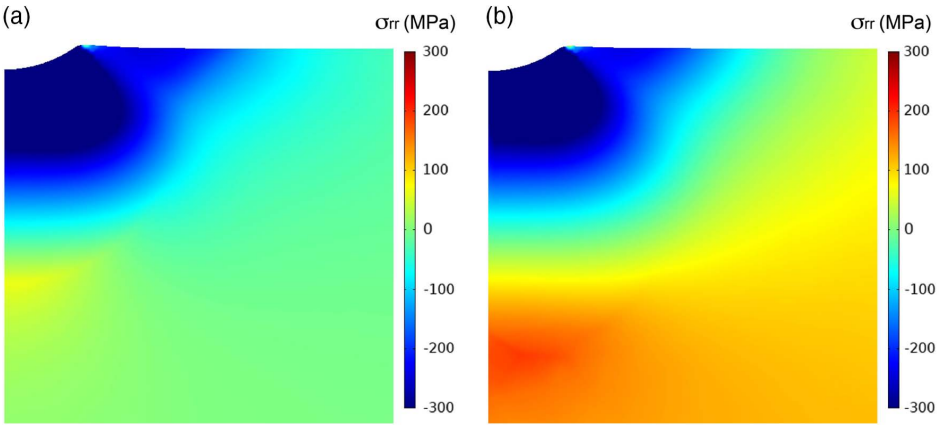

Figure 9. FEM-predicted fields of radial stress, under an indentation load of 1 kN, with a prior radial residual stress of a) 0 and b) +115 MPa.

3.2.3. Iterative FEM to Infer Residual Stress Level

The procedure for inferring the applied (equal-biaxial) residual stress level from the indentation profile is one of running the model with a series of residual stress values, comparing measured and predicted profiles for each experimental case, and evaluating the misfit parameter, S_{red}, each time. The inferred level is the one with the smallest value of this parameter. As there is only one parameter to infer, the convergence—i.e., the systematic movement in parameter space—can be achieved from a simple linear plot. For each applied residual stress level, this procedure was conducted for several different indentation loads. This was done in the same location in each case—i.e., a load was applied and removed, the profile was measured, and then a higher load was applied and the process repeated. The outcome of this operation is shown in **Figure 10**, for four values of the indentation load P.

Ideally, sharp minima in S_{red} would be observed for each curve at the actual applied residual stress level to which the curve is referred to. It can be seen that there are minima, and they do exhibit a broad trend of increasing inferred stress levels as the actual level is increased. On the other hand, many of the minima are not very sharp (indicating relatively poor sensitivity) and the agreement between inferred and actual levels is not close, particularly for the higher levels of applied load. This correlates with the residual indent profiles shown in Figure 7, where the influence of the residual stress level is seen to be lower for the higher applied load. The outcome is shown in **Figure 11**, which plots inferred stress levels against the corresponding actual levels.

The trends shown in Figure 11 are reasonably consistent and this could be taken to be encouraging. However, in detail, the outcomes highlight a number of difficulties. The sensitivity of an indent profile to the residual stress level is actually quite low, particularly for deeper penetration and for compressive stresses. This can be seen from the shape of these plots and the fact that the minimum S_{red} values are in many cases fairly high. (A value of the order of 10^{-4} or below represents good agreement.) This translates into a potential for large errors—probably of the order of ±100%. This is unlikely to be considered to be of much value.

4. Effects of Residual Stress on PIP Outcomes

4.1. For the Copper Used Experimentally

In many ways, the more important issue is not so much whether residual stresses can be accurately measured in this way, but whether the (unknown) presence of residual stress is likely to create large errors in inferred plasticity characteristics. (Of course, the two questions are linked, as both depend on the sensitivity of the residual indent profile to the presence of residual stresses.) This issue can be addressed via FEM modeling, with no real need for experimental data. It is done here first for the copper used in the experimental work, with the case of a harder material, exhibiting greater work hardening, being examined in the next section.

The logical way to explore this issue is to use the appropriate Voce parameter set (shown in Table 1), run FEM simulations with different levels of (equal-biaxial) residual stress (creating an indent profile in each case), and then, treat this profile as an experimental outcome and conduct the standard inverse procedure on it, so as to infer a new Voce set. One outcome of this is shown in **Figure 12**, for two applied loads (depths of penetration) and one magnitude of residual stress (just below the yield stress), both tensile and compressive. Figure 12 shows the indent profiles. For the unstressed cases, the initial and the inferred profiles are the same—they are for the same Voce set. For the residually stressed cases, on the other hand, both the predicted profile and the one for the best fit Voce set (neglecting residual stress) are shown. Certain features are clear. First, the relative shifts of the stressed profiles, compared with the unstressed ones, are greater for the lower load (as shown experimentally in Figure 7 and discussed in Section 3.2.2). Second, the shift is greater for tensile residual stresses than for compressive ones. Third, very close fit is not really achievable for the stressed cases—i.e., the effect of the residual stress cannot be closely replicated by simply changing the Voce set. Of course, in practice, this "error" will be convoluted in some way with the error associated with the experimental measurements.

Figure 13 shows a more practical perspective on these outcomes, showing the values of σ_Y and σ_{UTS} that would be obtained via this procedure—conversion of the Voce sets to these

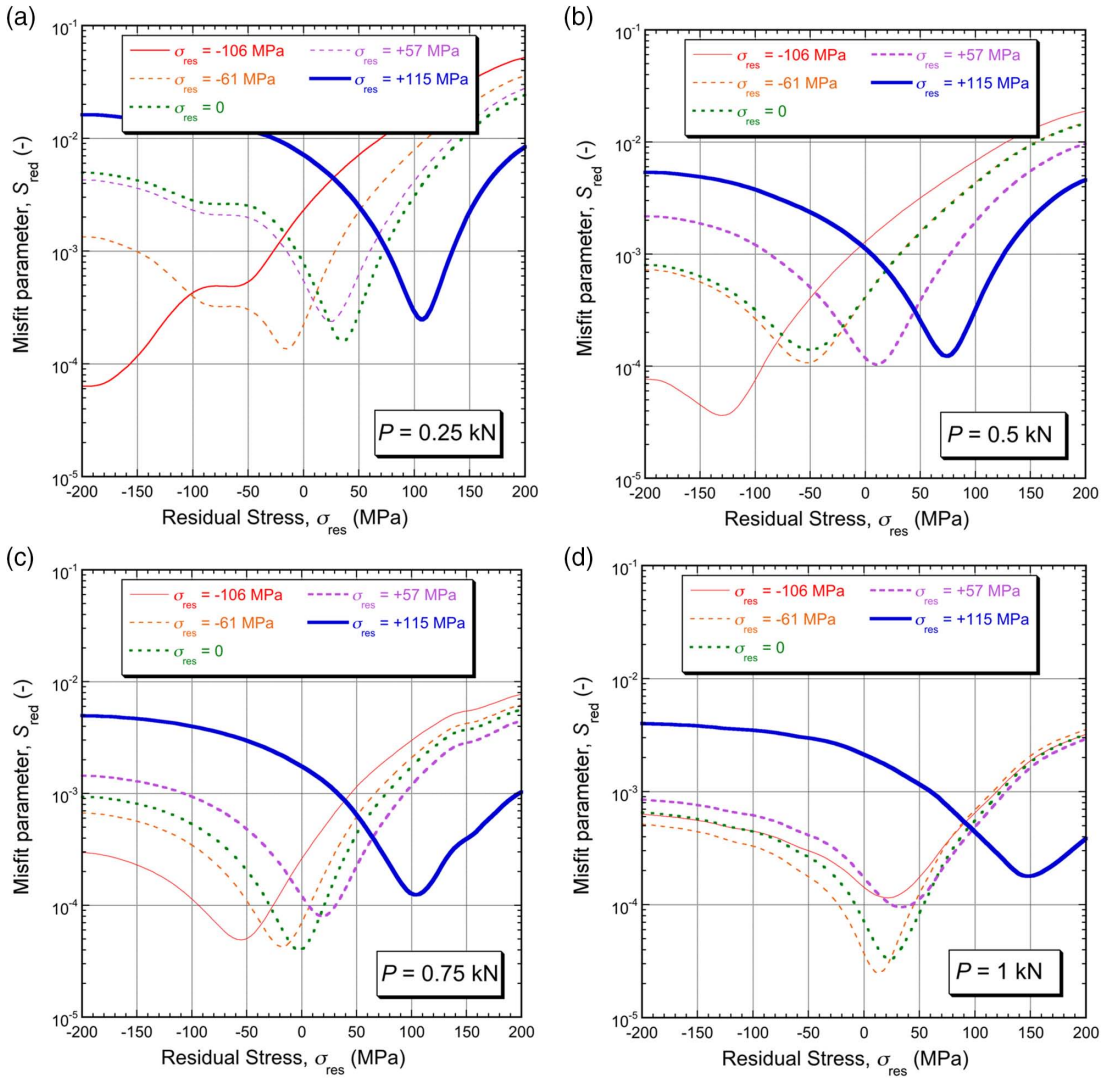

Figure 10. Plots of the misfit parameter as a function of the residual stress level assumed in the model, for five actual residual stresses and for indentation loads of: a) 0.25 kN, b) 0.5 kN, c) 0.75 Kn, and d) 1.0 kN.

properties hopefully assists interpretation. As each case corresponds to a set of three values (rather than a single residual stress value in Figure 10), these plots are not made up of discrete lines (for each residual stress level) but rather a cluster of S_{red} values. Nevertheless, the minimum S_{red} case for each residual stress level can be seen, giving the values of σ_Y and σ_{UTS} that would be obtained. Of course, with zero residual stress, these values are the "correct" ones.

Key features can again be seen. First, the sensitivity (i.e., the displacement to "incorrect" inferred values by the residual stress) is greater for shallow penetration (low δ/R). With $P = 0.25$ kN (for which $\delta/R \approx 4$–5%), the "correct" σ_Y of 200 MPa was moved to below 100 MPa by the tensile residual stress and up to about 250 MPa by the compressive one, whereas the corresponding values for $P = 1$ kN ($\delta/R \approx 18$–20%) are about 150 and 220 MPa. For the σ_{UTS} values, the displacements are lower and in the opposite directions, although the rather flat "curves" for the $P = 0.25$ kN case are indicative of poor resolvability. The "resolution" is better for the $P = 1$ kN case and the "displacements" (downward by a few MPa for the compressive stress and upward by about 20 MPa for the tensile one) are small.

As this relates to a high residual stress (relative to the yield stress, although not in absolute terms), these outcomes imply that in practice the errors in inferred stress–strain curves arising from the presence of residual stresses are likely to be quite small, particularly with deep penetration. Of course, this is consistent with the arguments in Section 3.2.2 and with Figure 9. It may again be noted that the sensitivity is greater for tensile stresses than for compressive ones. In practice, it is in fact rather more common for near-surface residual stresses to be compressive—for example, due to rolling, shot peening, etc.—which is advantageous in terms of being able to neglect their effects but a disadvantage if they are to be measured.

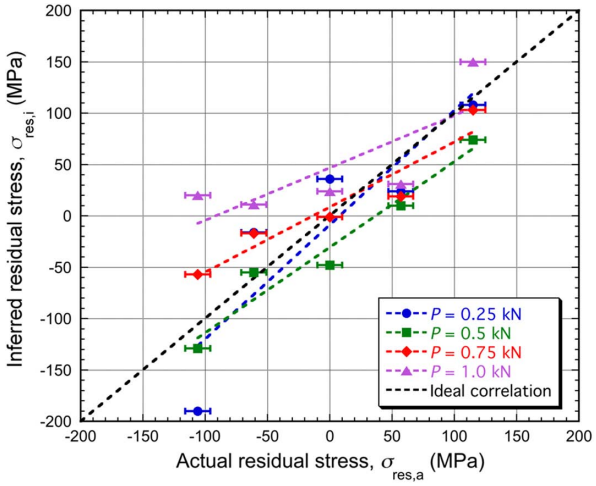

Figure 11. Summary outcome from the data in Figure 10, as a plot of the inferred level of residual stress against the actual value, for four indentation loads.

4.2. For a Harder Material

The data in Figures 12 and 13 suggest that, at least for deep penetration ($\delta/R > \approx 20\%$), the residual stress-induced errors in inferred plasticity parameters will usually be small ($< \approx 10\%$). However, this analysis refers to a relatively soft material (exhibiting little work hardening). For a material with a higher yield stress, the magnitude of the residual stress could be considerably greater, and it might be expected that this could lead to more significant changes in the residual indent profile, and hence in the inferred plasticity characteristics. **Figure 14** shows an analogous set of data to that of Figure 13, referring to a material (such as a Ni-based superalloy or fairly hard steel) with a yield stress several times greater than that of copper and also a higher work-hardening rate. (The two values of P in the plots give rise to δ/R values of about 4% and 20%, i.e., similar to those for the two lower loads in Figure 13.)

It can be seen that, while the trends and characteristics seen in these plots are similar to those of Figure 13, the effects are more significant. For example, even with deep penetration (Figure 14c), the presence of a tensile residual stress of 600 MPa has moved the inferred yield stress down from its correct value of 900 MPa to about 500 MPa. This is a high residual stress, the effects are weaker when they are compressive, and the errors induced in the UTS are much less pronounced. Nevertheless, these results do indicate that significant errors could arise in some cases. They also highlight the fact that it is the absolute magnitude of the residual stress that is important, rather than only the magnitude relative to the yield stress. (The 600 MPa level is actually a smaller fraction of the yield stress than is the 180 MPa level in Cu.) In other words, there is greater scope for error with harder metals (which at least have the potential to contain larger residual stresses than softer ones).

4.3. General Points

The data in Figures 13 and 14 can be used to highlight several points. Using relatively deep penetration (and 20% is actually a typical depth for PIP) will in general ensure that low-to-moderate levels of residual stress will have little or no effect on inferred plasticity characteristics. For harder materials, in which residual stress levels could be high (several hundred MPa or more), there is more danger of significant errors arising. For such cases, it might be advisable to conduct indentation to more than one depth: discrepancies between inferred sets of plasticity parameters from different depths could be indicative of the presence of residual stresses (with the parameter set obtained, using the deepest penetration, being likely to be the most accurate).

The capability for extracting plasticity characteristics in this way, even if residual stresses are present, is clearly an important one. An example is that of welds, which often have very different plasticity characteristics from those of the parent metal and also commonly contain residual stresses. As the dimensions of most welds make conventional (tensile) testing difficult, the use of PIP

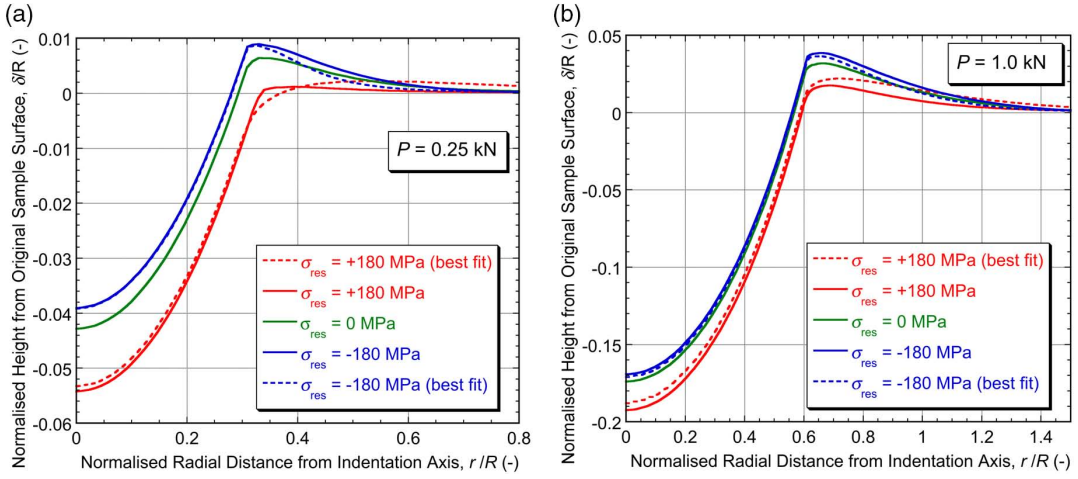

Figure 12. FEM-predicted indent profiles, with and without a prior residual stress of magnitude 180 MPa, for Cu, after loading to a) $P = 0.25$ kN and b) $P = 1.0$ kN.

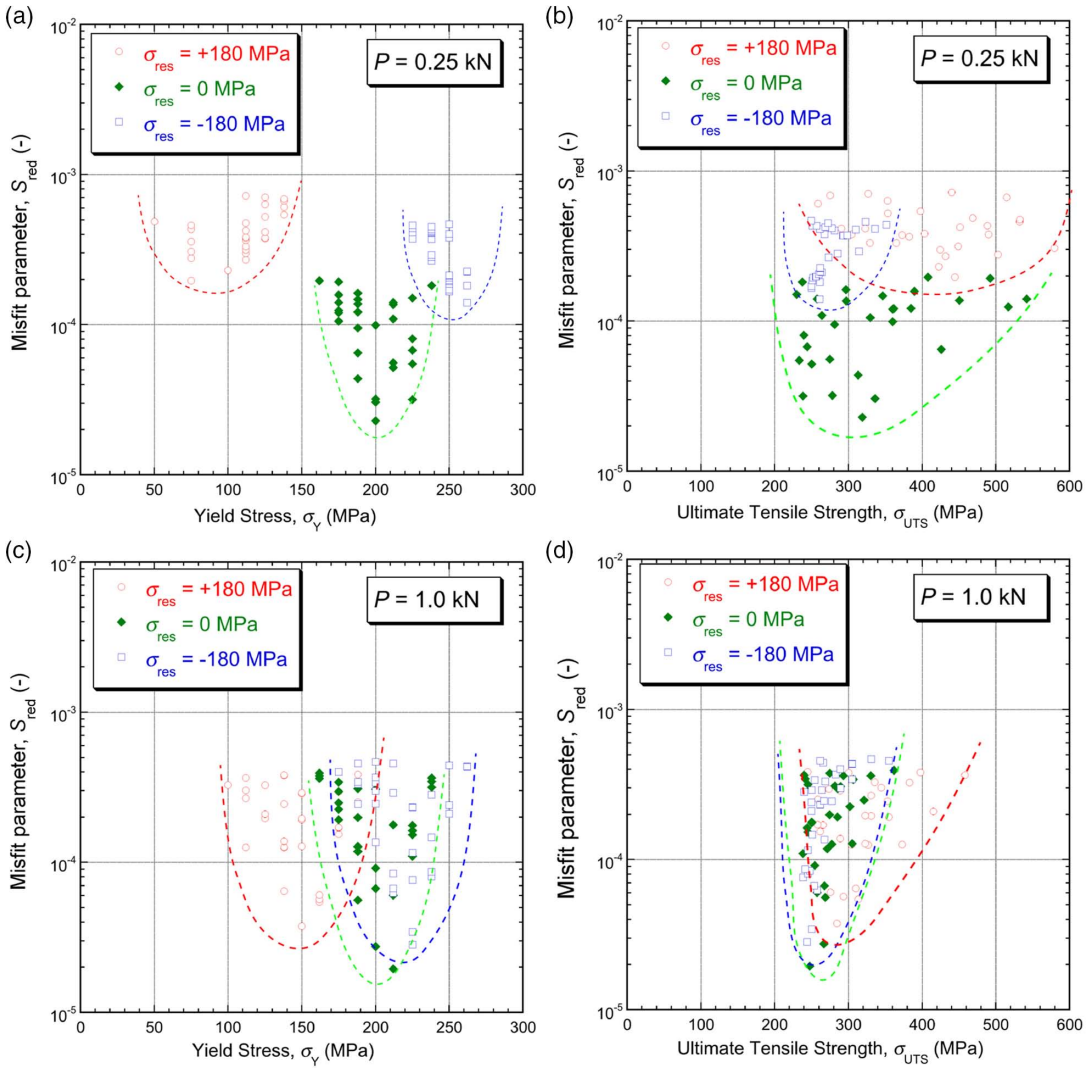

Figure 13. Scatter plots of S_{red} values for various Voce sets (with the "correct" set being the one in Table 1), characterizing the misfit between indent profiles obtained with and without residual stress. This is done both for shallow penetration ($P = 0.25$ kN), plotting against corresponding values of a) σ_Y and b) σ_{UTS}, and for deep penetration ($P = 1$ kN), plotting c) σ_Y and d) σ_{UTS}.

to obtain stress–strain curves for them, and even for different parts of a weld and for nearby HAZ regions, is very attractive.

The other key question concerns the prospects for using a PIP-type approach to measure residual stress levels. The results presented here clearly highlight that the sensitivities are not favorable for this. However, ensuring that the penetration is shallow does have the potential to improve them. It should be emphasized that this relates to the relative penetration (of a spherical indenter) and not to absolute depths. A figure of, say, 1–2% (i.e., about 10–20 μm depth with a 1 mm-radius sphere) could give fairly good sensitivity in terms of inferring the residual stress level (provided the plasticity characteristics are accurately known). However, shallow penetration brings its own problems, in terms of the necessary surface finish, the high resolution required for the depth measurement, etc. Also, in some cases, the indents may be located in single grains, leading to considerable scatter as a result of the dependence on grain orientation. In general, obtaining accurate residual stress levels in this way presents severe challenges, particularly if they are relatively low or are unequal biaxial.

5. Conclusions

The following conclusions can be drawn from this work. 1) Samples have been produced from 3 mm-thick copper sheet, in both cruciform shape and conventional dog-bone tensile test pieces. The cruciform samples were located in a loading frame, where they were subjected to a range of equal-biaxial loads (tensile and compressive) and then indented to various depths and the residual indent profiles measured. FEM simulation of the loading of these cruciform samples was used to relate the applied loads to the stress state induced in the sample in the (central) region to be indented. 2) The (true) stress–strain curve

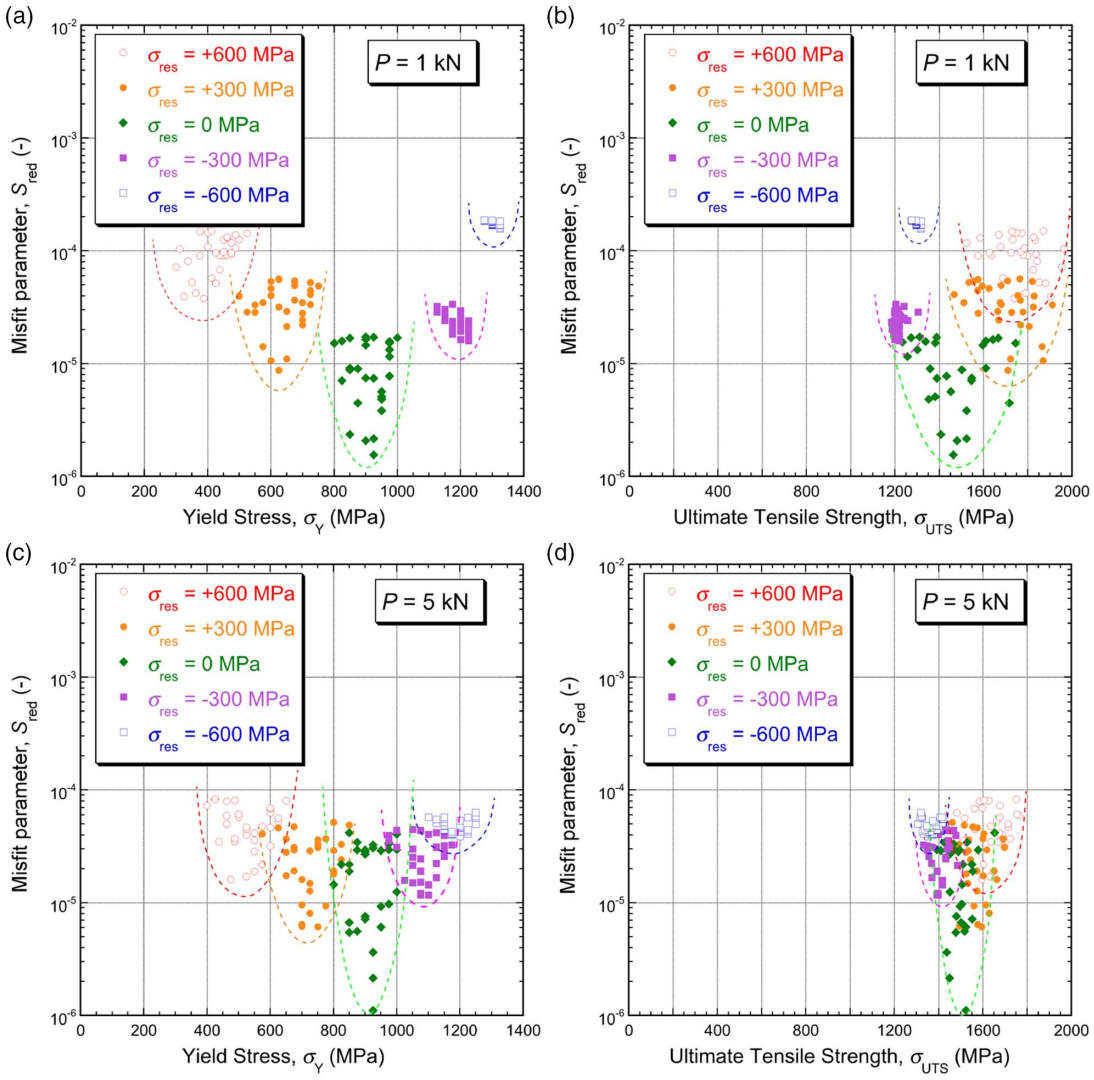

Figure 14. Analogous plots to those of Figure 13, for a material with a Voce parameter set of $\sigma_Y = 900$ MPa, $\sigma_s = 2300$ MPa, and $\varepsilon_0 = 20\%$ (giving $\sigma_{UTS} \approx 1480$ MPa).

of this material was obtained via indentation plastometry (involving iterative FEM simulation of the process) of the unstressed material. The outcome was in good agreement with that from conventional tensile testing, with a yield stress of about 200–220 MPa and a UTS of about 250 MPa. It was also confirmed that the material is isotropic. 3) A similar iterative procedure was applied to the experimental profiles produced with prior application of different levels of (radially symmetric) residual stress, seeking optimal agreement by varying the level of residual stress in the model. In this way, the inferred level of residual stress could be compared with the actual level imposed during the experiment concerned. 4) While there was very broad agreement between inferred and actual stress levels, in the sense that the trend was in the right direction, in detail, the agreement was poor. The reasons for this have been explored in some depth. The underlying reason is that the final profile exhibits very low sensitivity to the initial (residual) stress state, particularly with compressive stresses and for relatively deep penetration. More shallow penetration improves this sensitivity, although it may still be relatively poor, and very shallow penetration introduces other difficulties. 5) This low sensitivity of residual indent profiles to the presence of residual stresses, particularly for deep indenter penetration, does mean that the presence of unknown residual stresses is unlikely to introduce large errors into inferred plasticity parameters. This has been explored in some detail and it is concluded that significant errors could arise, particularly in the inferred yield stress, if very high residual stress levels are present (in relatively hard materials). If it is suspected that this may be the case, then indenting to more than one depth is suggested as a measure to check on this possibility.

Acknowledgements

Relevant support for TWC was received from EPSRC (grant EP/I038691/1) and from the Leverhulme Trust, in the form of an International Network Grant (IN-2016-004) and an Emeritus Fellowship (EM/2019-038/4).

Conflict of Interest

The authors declare no conflict of interest.

Data Availability Statement

Research data are not shared.

Keywords

indentation plastometry, inverse finite element method, residual stresses

Received: December 10, 2020
Revised: January 18, 2021
Published online: February 8, 2021

[1] T. H. Zhang, P. Jiang, Y. H. Feng, R. Yang, *J. Mater. Res.* **2009**, *24*, 3653.
[2] S. Pathak, S. R. Kalidindi, *Mater. Sci. Eng., R* **2015**, *91*, 1.
[3] Y. Z. Li, P. Stevens, M. C. Sun, C. Q. Zhang, W. Wang, *Int. J. Mech. Sci.* **2016**, *117*, 182.
[4] F. Pohl, *Exp. Tech.* **2018**, *42*, 343.
[5] C. Chang, M. A. Garrido, J. Ruiz-Hervias, Z. Zhang, L. L. Zhang, *Adv. Mater. Sci. Eng.* **2018**, *2018*, 1.
[6] J. Lee, C. Lee, B. Kim, *Mater. Des.* **2009**, *30*, 3395.
[7] W. Z. Yao, C. E. Krill, B. Albinski, H. C. Schneider, J. H. You, *J. Mater. Sci.* **2014**, *49*, 3705.
[8] M. Z. Wang, J. J. Wu, Y. Hui, Z. K. Zhang, X. P. Zhan, R. C. Guo, *Mater. Sci. Eng., A* **2017**, *679*, 143.
[9] J. E. Campbell, R. P. Thompson, J. Dean, T. W. Clyne, *Acta Mater.* **2019**, *168*, 87.
[10] C. Heinrich, A. M. Waas, A. S. Wineman, *Int. J. Solids Struct.* **2009**, *46*, 364.
[11] J. Dean, J. M. Wheeler, T. W. Clyne, *Acta Mater.* **2010**, *58*, 3613.
[12] D. K. Patel, S. R. Kalidindi, *Acta Mater.* **2016**, *112*, 295.
[13] J. Dean, T. W. Clyne, *Mech. Mater.* **2017**, *105*, 112.
[14] J. E. Campbell, R. P. Thompson, J. Dean, T. W. Clyne, *Mech. Mater.* **2018**, *124*, 118.
[15] L. Meng, P. Breitkopf, B. Raghavan, G. Mauvoisin, O. Bartier, X. Hernot, *Int. J. Mater. Form.* **2019**, *12*, 587.
[16] J. Isselin, A. Iost, J. Golek, D. Najjar, M. Bigerelle, *J. Nucl. Mater.* **2006**, *352*, 97.
[17] S. Swaddiwudhipong, J. Hua, E. Harsono, Z. S. Liu, N. S. B. Ooi, *Modell. Simul. Mater. Sci. Eng.* **2006**, *14*, 1347.
[18] I. Peyrot, P. O. Bouchard, R. Ghisleni, J. Michler, *J. Mater. Res.* **2009**, *24*, 936.
[19] J. Chen, H. N. Chen, J. Chen, *Acta Metall. Sin.* **2011**, *24*, 405.
[20] J. E. Campbell, T. Kalfhaus, R. Vassen, R. P. Thompson, J. Dean, T. W. Clyne, *Acta Mater.* **2018**, *154*, 237.
[21] Y. T. Tang, J. E. Campbell, M. Burley, J. Dean, R. C. Reed, T. W. Clyne, *Materialia* **2021**, *15*, 101017.
[22] J. E. Campbell, H. Zhang, M. Burley, M. Gee, A. T. Fry, J. Dean, T. W. Clyne, *Adv. Eng. Mater.* **2021**, unpublished.
[23] J. G. Swadener, B. Taljat, G. M. Pharr, *J. Mater. Res.* **2001**, *16*, 2091.
[24] Y. P. Cao, J. Lu, *Acta Mater.* **2004**, *52*, 4023.
[25] A. Yonezu, Y. Kuwahara, K. Yoneda, H. Hirakata, K. Minoshima, *Comput. Mater. Sci* **2009**, *47*, 611.
[26] J. Dean, G. Aldrich-Smith, T. W. Clyne, *Acta Mater.* **2011**, *59*, 2749.
[27] N. A. Sakharova, P. A. Prates, M. C. Oliveira, J. V. Fernandes, J. M. Antunes, *Strain* **2012**, *48*, 75.
[28] L. Shen, Y. M. He, D. B. Liu, Q. Gong, B. Zhang, J. Lei, *J. Mater. Res.* **2015**, *30*, 1078.
[29] P. L. Larsson, *J. Mater. Eng. Perform.* **2017**, *26*, 3854.
[30] T. H. Zhang, C. Yu, G. J. Peng, Y. H. Feng, *MRS Commun.* **2017**, *7*, 221.
[31] T. H. Pham, S. E. Kim, *Mater. Sci. Eng., A* **2017**, *688*, 352.
[32] G. J. Peng, Z. K. Lu, Y. Ma, Y. H. Feng, Y. Huan, T. H. Zhang, *J. Mater. Res.* **2018**, *33*, 884.
[33] Z. Y. Wang, L. X. Deng, J. P. Zhao, *Mater. Res. Express* **2019**, *6*, 036512.
[34] T. H. Zhang, W. Q. Cheng, G. J. Peng, Y. Ma, W. F. Jiang, J. J. Hu, H. Chen, *MRS Commun.* **2019**, *9*, 360.
[35] G. J. Peng, F. G. Xu, J. F. Chen, H. D. Wang, J. J. Hu, T. H. Zhang, *Metals* **2020**, *10*, 440.
[36] T. Akahori, T. Nagakura, S. Fushimi, A. Yonezu, *Polym. Test.* **2018**, *70*, 378.
[37] R. Moharrami, M. Sanayei, *Measurement* **2020**, *158*, 10.